Archives of Biochemistry and Biophysics 519 (2012) 46–58

Contents lists available at SciVerse ScienceDirect

Archives of Biochemistry and Biophysics

journal homepage: www.elsevier.com/locate/yabbi

On the stability of the extracellular hemoglobin of *Glossoscolex paulistus*, in two iron oxidation states, in the presence of urea

Francisco Adriano O. Carvalho [a], Patrícia S. Santiago [a,b], Marcel Tabak [a,*]

[a] Instituto de Química de São Carlos, Universidade de São Paulo, Sao Paulo, SP, Brazil
[b] Universidade Estadual Paulista "Júlio de Mesquita Filho" Registro, Sao Paulo, SP, Brazil

ARTICLE INFO

Article history:
Received 10 November 2011
and in revised form 4 January 2012
Available online 24 January 2012

Keywords:
Urea
Optical absorption
Fluorescence emission
Circular dichroism
Glossoscolex paulistus
Three-state model and oligomeric stability

ABSTRACT

The stability of the *Glossoscolex paulistus* hemoglobin (HbGp), in two iron oxidation states (and three forms), as monitored by optical absorption, fluorescence emission and circular dichroism (CD) spectroscopies, in the presence of the chaotropic agent urea, is studied. HbGp oligomeric dissociation, denaturation and iron oxidation are observed. CD data show that the cyanomet-HbGp is more stable than the oxy-form. Oxy- and cyanomet-HbGp show good fits on the basis of a two state model with critical urea concentrations at 220–222 nm of 5.1 ± 0.2 and 6.1 ± 0.1 mol/L, respectively. The three-state model was able to reveal a subtle second transition at lower urea concentration (1.0–2.0 mol/L) associated to partial oligomeric dissociation. The intermediate state for oxy- and cyanomet-HbGp is very similar to the native state. For met-HbGp, a different equilibrium, in the presence of urea, is observed. A sharp transition at 1.95 ± 0.05 mol/L of denaturant is observed, associated to oligomeric dissociation and hemichrome formation. In this case, analysis by a three-state model reveals the great similarity between the intermediate and the unfolded states. Analysis of spectroscopic data, by two-state and three-state models, reveals consistency of obtained thermodynamic parameters for HbGp urea denaturation.

Introduction

The extracellular hemoglobin of *Glossoscolex paulistus* (HbGp) has a molecular mass of 3.6 MDa, determined recently by analytical ultracentrigugation (AUC, [1]). This protein has an oligomeric structure composed by 144 globin chains, and 36 additional chains lacking the heme group, named linkers, similar to the orthologous *Lumbricus terrestris* hemoglobin (HbLt) [2]. Mass spectrometry and analytical ultracentrifugation studies suggest that HbGp has the same stoichiometry as HbLt, based on the Vinogradov model, which assumes that the whole protein is composed by 12 protomers, constituted by a dodecamer of globin chains and a trimer of linkers, $[(\boldsymbol{abcd})_3\boldsymbol{L}_3]$ [3–5]. Here ***a***, ***b***, ***c*** and ***d*** are globin chains forming an asymmetric tetramer ***abcd***, composed of a disulfide bonded trimer ***abc*** and a monomeric subunit ***d***. Three linker chains, $\boldsymbol{L}_1$, $\boldsymbol{L}_2$ and $\boldsymbol{L}_3$ complete the native protomer structure.

This class of proteins has a high resistance to oxidation and a high oligomeric stability when subjected to conditions of stress such as high temperature, pH variation, and addition of chemical agents (such as urea and surfactants), as compared, for instance, with human hemoglobin. These properties make them an interesting and important system for investigation [6,7], being also an advantage in biomedical applications. In this context, a strong motivation to study these giant hemoglobins is related to their potential use as blood substitutes. Studies have been performed in the past for HbLt [5], and are presently underway to test and validate the use of *Arenicola marina* hemoglobin (HbAm) in this direction [8,9].

The partial characterization of HbGp molecular mass (*MM*) by matrix assisted laser desorption time-of-flight mass spectrometry (MALDI-TOF-MS) confirmed the similarity of its subunits to those of orthologous proteins of this class, mentioned above [4]. This characteristic multi-subunit content confers to the whole protein a double-layered hexagonal oligomeric structure [10,11]. These extracellular hemoglobins are composed of a large number of subunits containing heme groups with *MM* in the range 15–19 kDa. These heme-containing subunits form monomers of 16 kDa (***d***) and disulfide bound hetero-trimers of 51–52 kDa (***abc***), linked by non-heme structures (24–32 kDa), named linkers (***L***) [3–5].

Analytical ultracentrifugation studies of HbGp, at pH 10.0, show that the whole oligomer dissociates into monomer subunit ***d***, dimer of monomers ***d***, $\boldsymbol{d}_2$, trimer ***abc***, and tetramer ***abcd***. However, for cyanomet-HbGp besides the appearance of these subunits, some fraction of un-dissociated whole protein is observed (17%), due to the fact that the cyanomet-form is more stable than oxy-HbGp, at pH 10.0 [5]. Studies by dynamic light scattering (DLS) of the HbGp as a function of temperature, at pH 7.0, show that oxy-HbGp is quite stable and no dissociation occurs up to a critical temperature, around 52 °C, where the protein undergoes

* Corresponding author. Fax: +55 16 3373 9982.
E-mail address: marcel@sc.usp.br (M. Tabak).

0003-9861/$ - see front matter © 2012 Elsevier Inc. All rights reserved.
doi:10.1016/j.abb.2012.01.007

denaturation with further aggregation at higher temperatures [12]. Besides that, differential scanning calorimetry (DSC) shows a single cooperative transition with a well defined endotherm. Cyanomet-HbGp is more stable as compared to oxy-HbGp based on its higher critical denaturation and dissociation temperatures, as observed from the DSC melting curves [12].

It has been known for many years that proteins can be unfolded in aqueous solution by high concentrations of certain reagents such as guanidine hydrochloride or urea. Denaturation with these chemicals is one of the primary ways of measuring the conformational stability of proteins and comparing the stability of mutant proteins [13,14]. In comparison to either acid or thermal unfolding, chemical agents such as urea and GuHCl are more effective in disturbing the non-covalent interactions. The extent of unfolding is generally greater than that of any other means of denaturation [13–16]. Despite their widespread use, the mode of action of these agents on protein conformation is not yet clearly known.

In this paper, we report on the study of the oligomeric stability of different forms of HbGp, in the presence of different concentrations of urea. This study was performed using several optical spectroscopic techniques to monitor the process of oligomeric dissociation and denaturation. The optical absorption spectroscopy was used for monitoring the changes in the vicinity of the heme group. Fluorescence emission and circular dichroism (CD)[1] spectroscopies were used to monitor changes in tertiary and secondary structures, respectively. The CD, fluorescence emission and light scattering intensity (LSI) data were used to calculate the Gibbs free energy and critical urea concentrations [$D_{1/2}$]. Analysis based on two-state and three-state models allowed to estimate thermodynamic parameters for the unfolding process, in the presence of urea.

Materials and methods

Protein extraction and purification

G. paulistus annelid is prevalent in sites near Piracicaba and Rio Claro cities in the state of São Paulo, Brazil. The hemoglobin of *G. paulistus* (HbGp) was prepared using freshly drawn blood from worms. HbGp solution was centrifuged at 2500 rpm for 15 min, at 4 °C. The sample was filtered (Mw cut-off 30 kDa) and centrifuged at 250,000*g*, at 4 °C, for 3 h. The pellet was resuspended in a minimum amount of 0.1 mol/L Tris–HCl buffer, at pH 7.0. Chromatography at pH 7.0 in a Sephadex G-200 column furnished the samples used in the experiments [17–19]. All concentrations were determined spectrophotometrically in a UV-1601 PC, Shimadzu spectrophotometer, using the appropriate molar absorption coefficients [17,20]. The final protein concentration in our stock solution was in the range 15–30 mg/mL in Tris–HCl 0.1 mol/L buffer, pH 7.0. In order to obtain the oxidized met-HbGp, a 5-fold molar excess of potassium ferricyanide relative to heme was added followed by 2-h incubation. To obtain the cyanomet-HbGp form, the met-HbGp was further incubated with a 5-fold molar excess of potassium cyanide relative to the heme. Excess of oxidants was removed by dialysis against the same buffer for 3 h.

All concentrations were determined spectrophotometrically using the molar extinction coefficients $\varepsilon_{415\ nm} = 5.5 \pm 0.8\ (mg/mL)^{-1}\ cm^{-1}$ for oxy-HbGp, $\varepsilon_{402\ nm} = 4.1 \pm 0.7\ (mg/mL)^{-1}\ cm^{-1}$ for met-HbGp and $\varepsilon_{420\ nm} = 4.8 \pm 0.5\ (mg/mL)^{-1}\ cm^{-1}$ for cyanomet-HbGp [17,21].

Spectroscopic measurements

Absorption spectra between 700 and 250 nm were measured, at 25 °C in a UV-1601 PC spectrophotometer (Shimadzu, Tokyo, Japan). Fluorescence emission measurements of HbGp in different conditions were carried out on a F-4500 spectrofluorimeter (Hitachi, Tokyo, Japan). All measurements were made at 25 °C using the pure buffer solution for baseline correction of the fluorescence intensity. The intrinsic protein fluorescence was recorded in the wavelength range from 305 to 450 nm, and the excitation wavelength was set at 295 nm. The slit widths for excitation and emission were set at 2.5 and 5.0 nm, respectively. Light scattering intensity (LSI) was measured in the F-4500 spectrofluorimeter (Hitachi, Tokyo, Japan) using both excitation and emission wavelengths at 350 nm.

In this work, fluorescence emission, optical absorption and light scattering intensity (LSI) experiments were performed on the three forms of HbGp, oxy-, cyanomet- and met-, exposed to 0.0–8.0 mol/L of urea. The samples were prepared in acetate–phosphate 20 mmol/L buffer, at 0.1 mg/mL concentration of protein.

Circular dichroism (CD) measurements were carried out using the Jasco J-810 spectropolarimeter (JASCO, Tokyo, Japan), at 25 °C. The CD spectra were obtained for two different spectral regions corresponding to the peptide bonds (213–250 nm) and heme groups and aromatic aminoacids (250–500 nm), with 1 mm path length cell. In the peptide bonds region a scan speed of 100 nm/min was used, with a band-width of 0.5 nm, and spectra were taken as an average of eight scans. In the heme groups region a scan speed of 200 nm/min was employed, with a band-width of 0.5 nm, and spectra were taken as an average of six scans. The protein concentrations used in the peptide bonds and heme regions were 0.3 and 3.0 mg/mL, respectively. The protein was exposed to 0.0–8.0 mol/L of urea. In each unfolding titration experiment the appropriate volume of buffer and stock urea were mixed to achieve the desired urea concentration (0.0–8.0 mol/L) in a final volume of 1 mL, prior to the addition of a constant aliquot of concentrated protein solution, to give the desired final concentration. The background from the buffer solution was subtracted for all the measurements of optical absorption, LSI, fluorescence emission and CD. The urea concentration at 25 °C was estimated by the empirical formula suggested by Pace [14].

$$[\mathrm{Urea}] = 117.66\ (\Delta n) + 29.753\ (\Delta n)^2 + 185.56\ (\Delta n)^3 \quad (1)$$

where Δn is the difference between the refractive index of the urea solution and of the buffer. All samples were incubated with urea for 2 h, at 25 °C, to reach equilibrium before measurements were performed.

Convex Constraint Algorithm (CCA)

The Convex Constraint Algorithm (CCA) software, developed by Perczel and Fasman [22], is commonly used in protein CD spectra deconvolution to estimate secondary structure contributions. In the present work, the CCA program was used to analyze the optical absorption spectra, aiming to obtain an estimate of the number of species in equilibrium, as a function of urea concentration, their individual fractional contribution of the total and their corresponding optical absorption spectra [18].

[1] *Abbreviations used:* CD, circular dichroism; cyanomet-HbGp, *Glossoscolex paulistus* hemoglobin with the iron in the ferric state coordinated to cyanide ion (CN^-); *D*, denaturant molarity (urea); $D_{1/2}$, critical denaturant molarity (urea); ΔG_U, unfolding free energy; ΔG_{H_2O}, protein conformational stability free energy; f_U, fraction of denatured protein; HbGp, *Glossoscolex paulistus* hemoglobin; HbLt, *Lumbricus terrestris* hemoglobin; hemichrome, coordination complex of heme iron in the ferric state, with the distal histidine in the sixth coordination position; LSI, light scattering intensity; m, parameter that measures the dependence of ΔG on denaturant molarity; *MM*, molecular mass; met-HbGp, *Glossoscolex paulistus* hemoglobin with the iron in the ferric state coordinated to water; oxy-HbGp, *Glossoscolex paulistus* hemoglobin with the iron in the ferrous state coordinated to oxygen.

The CCA method is a general spectral decomposition procedure based on the simplex algorithm. It calculates a variable number p of base functions f_i (pure spectra corresponding to different species in equilibrium) and the respective coefficients C_{ij} in the linear combination of functions f_i, for recovering the functions f_j (experimental spectra) [18,22]:

$$f_i = \sum_{i=1}^{p} C_{ij} f_i \tag{2}$$

Three constraints upon these coefficients are imposed: (1) the sum of the coefficients is unity for each value of j, $\Sigma\, C_{ij} = 1$, where $j = 1,2,\ldots,N$, and N is the number of experimental functions (experimental spectra) in the analysis. (2) The coefficients are all positive, $C_{ij} > 0$. (3) The points corresponding to C_{ij} comply with a simplex in the Euclidian space of dimension p with the minimal volume. A full description and examples of this procedure are given in literature [18,22].

Analysis of denaturation equilibrium

The study of the equilibrium between the folded and unfolded conformations requires destabilizing the protein so that both conformations are present at measurable concentrations. The folded state in water is favored when compared to the unfolded state [14,15]. However, the equilibrium can be displaced to the unfolded state by addition of denaturant agent. Urea is a chemical agent which is often used to induce protein denaturation and thus to assess protein stability [15].

Two-state folding model

The denaturation plots were made based on the ellipticity of the native and unfolded HbGp, at several characteristic wavelengths, as a function of denaturant concentration. Further analysis of the data by a two-state model was performed as described in Ref. [14]. It is assumed that at 0.0 mol/L of urea the protein is totally in the native state, while at 8.0 mol/L of denaturant it is in the unfolded state. For a protein denaturation mechanism, based on the two-state model, the fraction of protein denaturation (f_U) can be expressed by the Eq. (3) below [23,24]:

$$f_U = \frac{\theta_N - \theta_X}{\theta_N - \theta_D} \tag{3}$$

where θ_X is the observed value of the ellipticity at a given denaturant concentration, and θ_N and θ_D are the ellipticity values of native and unfolded protein states, respectively [23,24]. For a two-state mechanism, the equilibrium constant, K, can be calculated using the Eq. (4) [23,24]:

$$K = \frac{f_U}{f_N} = \frac{f_U}{1 - f_U} = \frac{\theta_N - \theta_X}{\theta_X - \theta_D} \tag{4}$$

The Gibbs free energy is related with the equilibrium constant (K) by the Eq. (5):

$$\Delta G_U = -RT\ \ln K \tag{5}$$

where R is the gas constant and T is the absolute temperature. It is assumed that the free energy of unfolding, ΔG_U, has a linear dependence on the concentration of the denaturant agent, in this case, urea [D].

$$\Delta G_U = \Delta G_{H_2O} - m[D] \tag{6}$$

ΔG_{H_2O} and m are, therefore, the intercept and slope, respectively, of the plot of ΔG_U versus [D]. ΔG_{H_2O} is an estimate of the conformational stability of the protein that assumes that the linear dependence continues to 0.0 mol/L of denaturant agent and m is a measure of the dependence of ΔG_U on the urea concentration, and is associated with the cooperativity of the unfolding reaction [24].

When the system is in equilibrium ($\Delta G_U = 0$) an urea concentration [D] corresponding to the critical concentration of denaturant agent is obtained [$D_{1/2}$].

In this work, the ellipticity changes, as a function of urea concentration, were fitted based on the two-state model by the sigmoidal fit described by Eq. (3). The fractions of denatured HbGp, in the oxy- and cyanomet-HbGp forms, were calculated, allowing the determination of the critical concentrations of urea, [$D_{1/2}$] [23,24]. From the denatured protein fractions (f_U), at several different wavelengths, the equilibrium constant (K) and Gibbs free energy for the denaturation process, ΔG_U, were estimated. The thermodynamic parameters described above were obtained by several independent techniques such as fluorescence emission, light scattering intensity (LSI) and circular dichroism, through the analysis of the corresponding data.

Three-state folding model

Analysis of the HbGp urea denaturation data, considering the whole range of experimental points, was also performed based on a three-state denaturation model. An assumption is made, that, upon unfolding, the protein in the native state (N) is in equilibrium with an intermediate (I) and the unfolded (U) states. The three-state model recognizes the presence of one stable intermediate structure (I), which is populated during the transition from the folded state (N) to the unfolded one (U) [25].

The Eq. (7) below shows a scheme of a three-state unfolding reaction, where the native and unfolded states are in equilibrium with an intermediary state [25,26].

$$N \rightleftarrows I \rightarrow U \tag{7}$$

The dependence of the observed signal with the denaturant concentration, for the three-state model, is given by the Eq. (8) [26].

$$y = \frac{y_N + y_L exp - \left[\frac{(\Delta G_1^0 - m_1[D])}{RT}\right] + y_U exp - \left[\frac{(\Delta G_1^0 + \Delta G_2^0 - (m_1 + m_2)[D])}{RT}\right]}{1 + exp - \left[\frac{(\Delta G_1^0 - m_1[D])}{RT}\right] + exp - \left[\frac{(\Delta G_1^0 + \Delta G_2^0 - (m_1 + m_2)[D])}{RT}\right]} \tag{8}$$

where y is the measured signal, y_N, y_I, y_U are the intercepts corresponding to the native, intermediate and unfolded states, respectively. m_1 and m_2 are the slopes of the pre- and post-transition baselines. ΔG_1 and ΔG_2 are, respectively, the differences in Gibbs' free energy of native and intermediate states due to the first transition ($N \rightarrow I$), and between intermediate and unfolded states due to the second transition ($I \rightarrow U$), and [D] is the denaturant concentration. R is the gas constant and T the absolute temperature in Kelvin. The *Origin* 8.0 program was used to analyze the denaturation curves by urea.

In general, in this analysis of denaturation data, two approximations are considered. The first case assumes that the physical property under study has similar or identical values for the native and intermediate states, $y_N = y_I$, while the second case considers that the intermediate and unfolded states are undistinguishable, $y_I = y_U$ [27].

The $[D]_{1/2}$ value can be determined as the ratio between the free-energy and the slopes of each transition, m_1 and m_2 as shown in the equations below [26].

$$([D]_{1/2})_1 = \Delta G_1^0/m_1 \text{ and } ([D]_{1/2})_2 = \Delta G_2^0/m_2 \tag{9}$$

Although the number of variables in the three-state model equation increases as compared to the two-state one, the use of the whole range of experimental points allows an accurate determination of the apparent thermodynamic parameters [28].

Reversibility of HbGp denaturation

The reversibility of the unfolding process for HbGp was tested by comparing the optical absorption and fluorescence emission spectra at several urea concentrations, after incubation of the samples for 2 h, at 25 °C. The urea was removed from the solutions by dialysis against phosphate 20 mmol/L buffer, for 6 h. The optical absorption and fluorescence emission spectra were measured, before and after the dialysis, and the results were compared to the spectra of native HbGp (0.0 mol/L of urea). The experiment to test the reversibility, used in this work, is described in detail in the literature for another protein (Chaperonin 10) [29].

Results and discussion

Optical absorption

Cyanomet-HbGp

The optical absorption spectra of HbGp were measured for reduced (Fe^{2+}, oxy-HbGp) and oxidized (Fe^{+3}, met- and cyanomet-HbGp) forms, as a function of urea concentration. The difference between the met- and cyanomet-HbGp forms is the ligand in the sixth coordination of the heme iron, that in the met-HbGp is a water molecule while in the cyanomet-HbGp is the cyanide ligand (CN^-).

In Fig. 1A the characteristic optical absorption spectra of cyanomet-HbGp, in the absence and in the presence of urea, with the Soret band maximum wavelength at 420 nm and Q bands at 540 nm, are shown. No significant changes in the absorption wavelength λ_{abs} of Soret band are observed, up to 4.0 mol/L, suggesting that, cyanomet-HbGp is quite stable at low urea concentrations (Table 1). However, the increase in urea concentration, above 4.0 mol/L, induces the decrease in intensity and the blue-shift of the Soret band (Table 1). For cyanomet-HbGp the blue-shift from 420 to 404 nm suggests changes in the heme iron with formation of some new species. At 8.0 mol/L of urea, absorption bands at 360, 404, 531, 567 and 631 nm are observed in the spectrum, suggesting a mixture of several species in equilibrium (Fig. 1B and C). The bands at 360, 404 and 631 nm are characteristic of aquomet- and penta-coordinated species and the bands at 531 and 567 nm are common for the hemichrome species. The band at 631 nm is common for high-spin species in iron complexes [30,31]. The penta-coordinated and hemichrome species are characterized by iron in the ferric state with coordination number of five and six, respectively. In the case of the hemichrome the sixth coordination is occupied by distal histidine.

In general the globins stability is attributed to the ligand coordinated to iron metal center. Studies suggest that the CN^- is a strong ligand and induces an increase in stability of proteins [32]. The further increase in the urea concentration, above 4.0 mol/L, induces significant structural disorder and changes in the native state, promoting oligomeric dissociation, protein denaturation and alteration in the coordination sphere of the heme iron. These results are in agreement with analytical ultracentrifugation data (AUC) and DLS, where the higher stability for the cyanomet-HbGp in the presence of other denaturant agents (alkaline pH) was observed [5,12]. Moreover, a report on the stability of human hemoglobin (Hb) suggested that the cyanomet-Hb form is the most stable and resistant to unfolding by urea, as compared to several other forms, such as deoxy-Hb, CO-Hb and oxy-Hb [30].

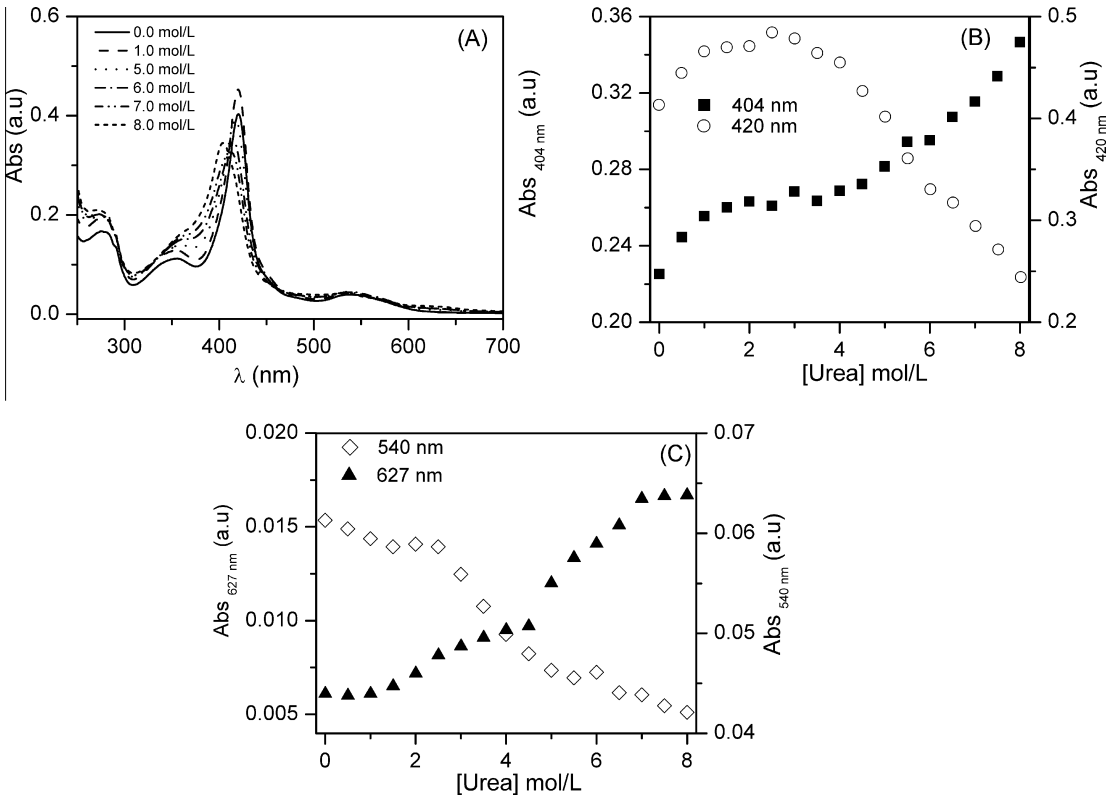

Fig. 1. (A) Optical absorption spectra of the cyanomet-HbGp 0.1 mg/mL, in 20 mmol/L of mixed acetate–phosphate buffer, in the presence of urea, at pH 7.0. (B) Absorbances at wavelengths 404 and 420 nm; and (C) absorbances at wavelengths 540 and 627 nm, as a function of the concentration of urea.

Table 1
Spectroscopic properties of the HbGp in presence of urea.

Forms	Properties	Urea concentration (mol/L)				
		0.0	2.0	4.0	6.0	8.0
Cyanomet-HbGp	λ_{abs} (nm)[a]	420	420	420	415	404
	Abs[b]	0.43	0.47	0.45	0.33	0.24
	λ_{max} (nm)[c]	333	333	340	348	350
	LSI	3240	3430	2130	780	780
Oxy-HbGp	λ_{abs} (nm)[a]	415	415	415	413	407
	Abs[b]	0.54	0.59	0.59	0.45	0.34
	λ_{max} (nm)[c]	333	334	343	348	350
	LSI	4050	2930	2225	975	980
Met-HbGp	λ_{abs} (nm)[a]	402	413	413	412	407
	Abs[b]	0.42	0.34	0.30	0.33	0.39
	λ_{max} (nm)[c]	333	336	338	346	351
	LSI	3150	780	1200	1100	780

[a] Soret band maximum wavelength.
[b] Absorbances in Soret band.
[c] Wavelength maximum emission.

Oxy-HbGp

Oxy-HbGp displays characteristic absorbances at 415, 540 and 576 nm, in the absence of urea. The absorption spectrum remains quite stable up to 4.0 mol/L of denaturant, suggesting that the iron environment in the heme group does not present measurable changes (Table 1). However, further increase in urea concentration promoted significant changes in the absorption spectra, similar to that observed for cyanomet-HbGp. The Soret and *Q* bands absorption intensities decrease and blue-shift from 415 to 407 nm, from 540 to 533 nm (alpha), and from 575 to 568 nm (beta), respectively (Table 1).

The absorption spectrum at 8.0 mol/L of urea corresponds to a mixture of several species, as deduced from the fact that the Soret band wavelength is shifted to around 407 nm and other less intense bands in the visible region are observed, at 533, 568 and 628 nm [21]. Thus, at higher urea concentration the denaturation process occurs with the oxidation of the iron from Fe^{+2} to Fe^{+3}, inducing the formation of several species [21]. The charge-transfer (CT) band gives important information about the strength of the axial ligands of the heme proteins. This transition is associated with the promotion of an electron from the highest filled porphyrin π orbitals to the e_g (d_{xz}, d_{yz}) orbitals of the iron atom. The band around 628–634 nm is characteristic of aquomet-species, where the water is coordinated in sixth coordination [33]. However, the bands at 533 and 568 nm are characteristic of a hemichrome species, so that at 8.0 mol/L of urea various species are detected and coexist in equilibrium. The oligomeric dissociation promoted the formation of several oxidized species, such as hemichrome and aquomet-HbGp: the dissociation and protein denaturation facilitate the access of water to the hydrophobic heme pocket. Literature studies show that oxy-myoglobin, in the presence of 8.0 mol/L urea, undergoes very rapid oxidation, with the formation of the hemichrome species [30]. The decreased heme absorption intensity is associated to the loss of protein structure (Table 1). Our results show that addition of urea has several effects upon oxy-HbGp, so that the increase of urea concentration induced the oxidation of the heme iron, together with the oligomeric dissociation and the protein denaturation.

Met-HbGp

Initially, in the absence of urea, the characteristic spectrum of the aquomet-HbGp is observed, with an intense broad Soret band centered at 402 nm, a *Q* band at 500 nm and another band at 627 nm (Fig. 2A and C). The met-HbGp presents an equilibrium, in the presence of urea, which is more complex as compared to oxy- and cyanomet-HbGp, with the formation of several species (at least three species, Fig. 2C and D). The addition of urea up to around 1.5–2.5 mol/L shows a red-shift of the Soret band from 402 to 413 nm (Fig. 2B), indicating that at low urea concentration the formation of a hemichrome species is promoted. This hemichrome species is characterized by a reddish brown solution and a narrow intense Soret band centered at 413 nm, and *Q* bands at 534 and 565 nm [21]. Moreover, the spectral changes are very significant with a marked decrease in the Soret band width. In this limited urea concentration range the band at 627 nm, characteristic of high-spin heme, is not observed, suggesting that the hemichrome is the single species in the solution. Further increase in urea concentration, above 5.0–6.0 mol/L, is accompanied by a blue-shift from 413 to 407 nm (Table 1), and a simultaneous increase of the absorbance at 627 nm, indicating that there is a mixture of species at 8.0 mol/L of urea [30,31].

In Fig. 2C and D the results of the analysis by the Convex Constraint Algorithm (CCA) [34] are shown for met-HbGp. Three species are observed in the equilibrium of met-HbGp, as a function of urea. Initially, only the aquomet-HbGp species is present up to 1.5 mol/L of urea. The midpoint of the first transition occurs around 1.0 mol/L of urea, where the aquomet- and hemichrome species are in equilibrium (Fig. 2D). At 1.5 mol/L of urea, the hemichrome species appears, giving 100% contribution in the urea concentration range from 2.0 to 3.5 mol/L (Fig. 2D). The maximum absorption of the Soret band does not undergo any drastic changes in the range from 2.5 to 5.5 mol/L urea, suggesting that the hemichrome is very stable, under these conditions (Fig. 2B). Moreover, further increase of the urea concentration induced the formation of the third species that is assigned to the protein in the denatured state, where a penta-coordinated species is the predominant one in solution. The second midpoint transition corresponds to an equilibrium between the hemichrome and the penta-coordinated species and occurs around 5.5 mol/L of urea (Fig. 2D). The high critical denaturant value for this second transition is attributed to the larger stability of the hemichrome species as compared to the aquomet-species.

Fluorescence emission

Fluorescence emission spectra for oxy-HbGp, at different urea concentrations, are presented in Fig. 3A, while the normalized (relative to 0.0 mol/L) total fluorescence for oxy-, met-, and cyanomet-forms is shown in Fig. 3B. A significant fluorescence increase,

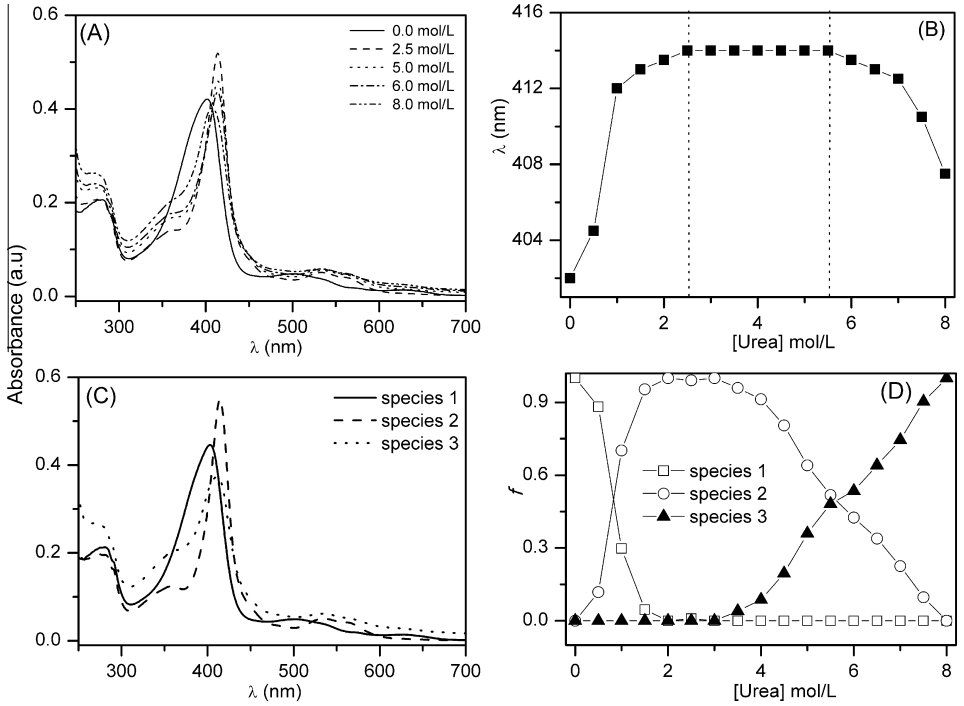

Fig. 2. (A) Optical absorption spectra of the met-HbGp 0.1 mg/mL, in 20 mmol/L of mixed acetate–phosphate buffer, in the presence of urea, at pH 7.0. (B) Soret band maximum wavelength, (C) absorption spectra corresponding to the species obtained by the decomposition of the full set of optical spectra in (A), carried out by means of the software CCA (see "Methods") and showing the three species in equilibrium. (D) Percentage contribution (fraction) of the species present in equilibrium shown in (C), as a function of the concentration of urea.

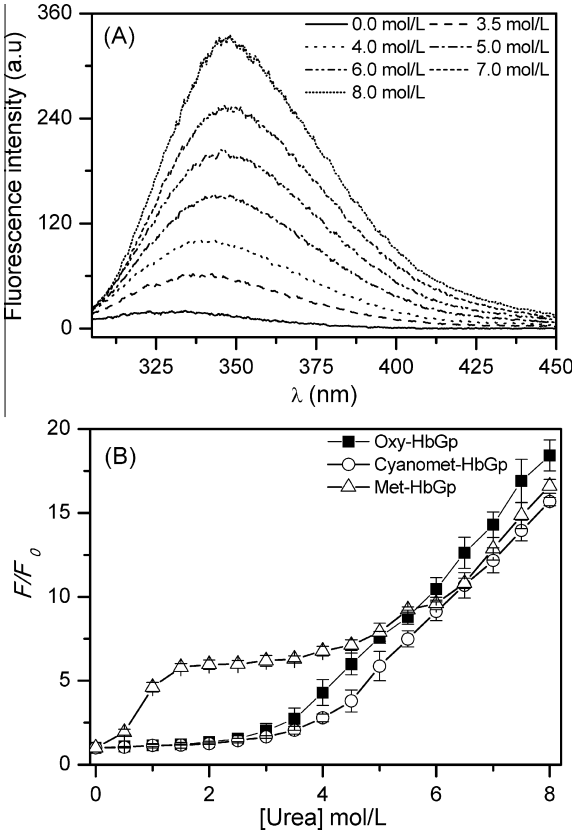

Fig. 3. (A) Fluorescence emission spectra for oxy-HbGp 0.1 mg/mL, in 20 mmol/L of mixed acetate–phosphate buffer, as a function of urea concentration. (B) Normalized (to the value in the absence of urea) total fluorescence emission area for the different HbGp oxidation species. Symbols correspond to average values ± standard deviation (SD) of three independent experiments.

around 18-fold, is observed for the oxy-, cyanomet- and met-HbGp forms, upon going from 0.0 to 8.0 mol/L of urea. The emission maxima for the three HbGp forms as a function of the urea concentration are shown in (Table 1). The pattern of λ_{max} changes is very similar for the three HbGp forms.

The oxy- and cyanomet-HbGp forms show similar processes of dissociation/denaturation, where florescence intensity remains constant up to 3.5 mol/L of urea, the cyanomet-HbGp being slightly more stable in the presence of urea (Fig. 3B). Above 4.0 mol/L of urea, due to the protein oligomeric dissociation, a more significant change in tryptophan emission λ_{max} is observed and a red-shift from 333 to 350 nm is noticed, consistent with both the reduction of the energy transfer from the tryptophans to the hemes, and the increase in exposure of the fluorophores to the solvent (Table 1, [20,21,23,35]). The small shift of the curve for cyanomet-HbGp to slightly higher urea concentrations is also an expected observation considering the high stability of this oxidation form of the protein (Table 1, [36]).

However, the met-form displays, a 6-fold fluorescence increase at 1.5 mol/L, remaining constant in the concentration range from 1.5 to 5.0 mol/L, then increasing around 18-fold at 8.0 mol/L of urea. The small changes in the concentration range between 1.0 and 3.5 mol/L, observed for met-HbGp, are due to the formation of the hemichrome species, as observed by optical absorption spectroscopy. The dissociation of the protein oligomeric structure leading to the removal of the significant quenching of the tryptophan fluorescence due to the energy transfer to the heme groups, both inter- and intramolecularly, is probably, the cause of this effect [35,36]. This energy-transfer phenomenon is a well-known effect in hemoglobins. The fluorescence results show that the addition of urea leads to dissociation and denaturation of the three HbGp forms, at 8.0 mol/L de urea, but the mechanism of dissociation/denaturation is different.

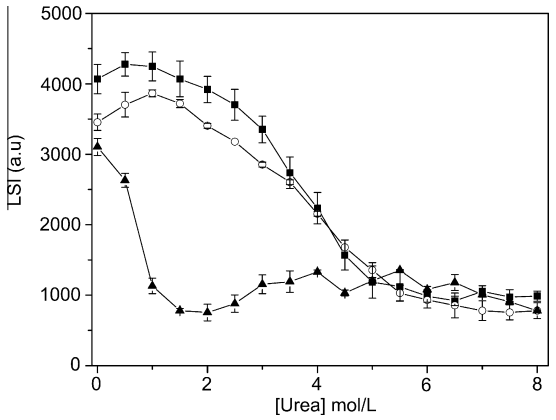

Fig. 4. Light scattering intensity (LSI) for the three forms of HbGp 0.1 mg/mL, as a function of urea concentration in the range from 0.0 to 8.0 mol/L, at pH 7.0. Oxy-HbGp (■), cyanomet-HbGp (○) and met-HbGp (▲). Symbols correspond to average values ± standard deviation (SD) of three independent experiments.

Light scattering intensity (LSI)

Light scattering intensity was monitored in the fluorimeter to evaluate the process of denaturation and dissociation of HbGp, in the three studied forms. Fig. 4 presents light scattering intensity data for the three HbGp forms, as a function of urea concentration, at pH 7.0. The oxy- and cyanomet-HbGp forms display similar curves, while the met-HbGp plot is very different, showing a decrease of intensity at lower urea concentrations. The cyanomet-HbGp displays a slightly smaller scattering intensity due to the fact that coordination of the CN^- ligand to the iron induces changes in the protein volume, as measured by the frictional parameter in ultracentrifugation studies [5]. The met-HbGp is more unstable and dissociated at lower urea concentrations [21]. Based on the optical absorption data described above, implying the formation of hemichrome at low urea concentrations, as well as on the increase in the fluorescence emission, overall, our results suggest that the formation of the hemichrome species by urea could trigger the destabilization of met-HbGp oligomeric structure. Moreover, the significant reduction in light scattering intensity observed for met-HbGp at 1.0 mol/L, while this phenomenon occurs for the other two forms at higher urea concentrations, around 4.0 mol/L, suggests that the urea induces first the protein oligomeric dissociation, followed by subsequent denaturation. Although the scattering intensity is an indirect measure of the oligomeric dissociation, this seems to be an adequate tool, since the light scattering intensity depends on the volume of the scattering particles in solution. Besides, data from size exclusion chromatography (SEC) have shown that, at 4.0 and 5.0 mol/L of urea, the oxy-HbGp is partially dissociated into smaller subunits, monomer ***d***, trimer ***abc*** and a remaining fraction of the whole protein (data not shown).

Circular dichroism (CD)

Oxy-HbGp

The reversibility of HbGp unfolding in the presence of urea was assessed according to the description presented in Reversibility of HbGp denaturation. Our results are shown in Fig. S1 of the Supporting information, and suggest that the HbGp denaturation process is only partly reversible. Thus, it is observed that, up to 4.0 mol/L of denaturant, after dialysis of the protein samples to remove urea, the spectral parameters are identical to those for oxy-HbGp, in the absence of urea (emission λ_{max} is 333 nm and Soret band is at 415 nm, see Table 1 and Fig. S1), suggesting a reversible process. However, the precipitation of HbGp, at 6.0 mol/L of urea, after dialysis, indicates that some hydrophobic residues were exposed upon denaturation. The subsequent removal of denaturant from the protein solution induced changes in these residues, leading to disordered association and precipitation. Fig. S1.C shows that a significant difference is observed for the maximum of absorption in the Soret band, before and after the dialysis, due to the partial protein precipitation induced by urea, above 4.0 mol/L. This phenomenon characterizes an irreversible unfolding. Therefore the HbGp unfolding can be considered as partly reversible.

In Fig. 5A and B circular dichroism (CD) spectra of oxy-HbGp in the peptide and heme group regions, respectively, in the presence of urea, from 0.0 to 8.0 mol/L, at pH 7.0, are shown. The CD spectra in the peptide region (Fig. 5A) present a region of negative ellipticity at 220–222 nm, characteristic of proteins which are rich in α-helix structure. In Fig. 5B two bands at 262 and 414 nm correspond, respectively, to the contributions of aromatic aminoacids and Soret band. Moreover, the Fig. 5B shows clearly that, up to 4.0 mol/L of urea, only small spectral changes are observed, while at 8.0 mol/L of denaturant the ellipticity is near zero, suggesting that the protein is completely denatured. The oxy-HbGp, in the presence of urea, is quite stable, up to 3.5–4.0 mol/L, without any drastic CD spectral changes. In Fig. 5A, due to the urea absorption, the CD spectral range was limited to wavelengths above 212 nm. The denaturation of HbGp was monitored through the analysis of the ellipticities at 222, 414, 260 and 334 nm to obtain a critical urea concentration $D_{1/2}$ and a Gibbs free energy for the protein denaturation process, using a two state model, described by the Eqs. (3)–(6) (see Methods section, [24,37–39]).

Two-state model. The HbGp unfolding reaction is quite complex due to the complexity of the protein oligomeric structure, consisting of 180 polypeptide chains. Thus, the analysis of the thermodynamic parameters, associated to the protein unfolding, was made

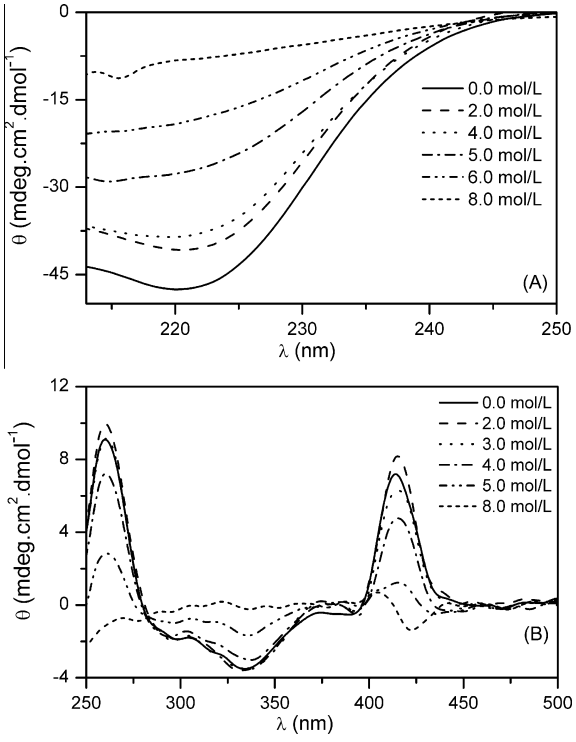

Fig. 5. CD spectra of oxy-HbGp in 20 mmol/L phosphate buffer, at pH 7.0, in the presence of urea in the range 0.0–8.0 mol/L. (A) peptide region at 0.3 mg/mL of protein and (B) Soret region at 3 mg/mL of protein.

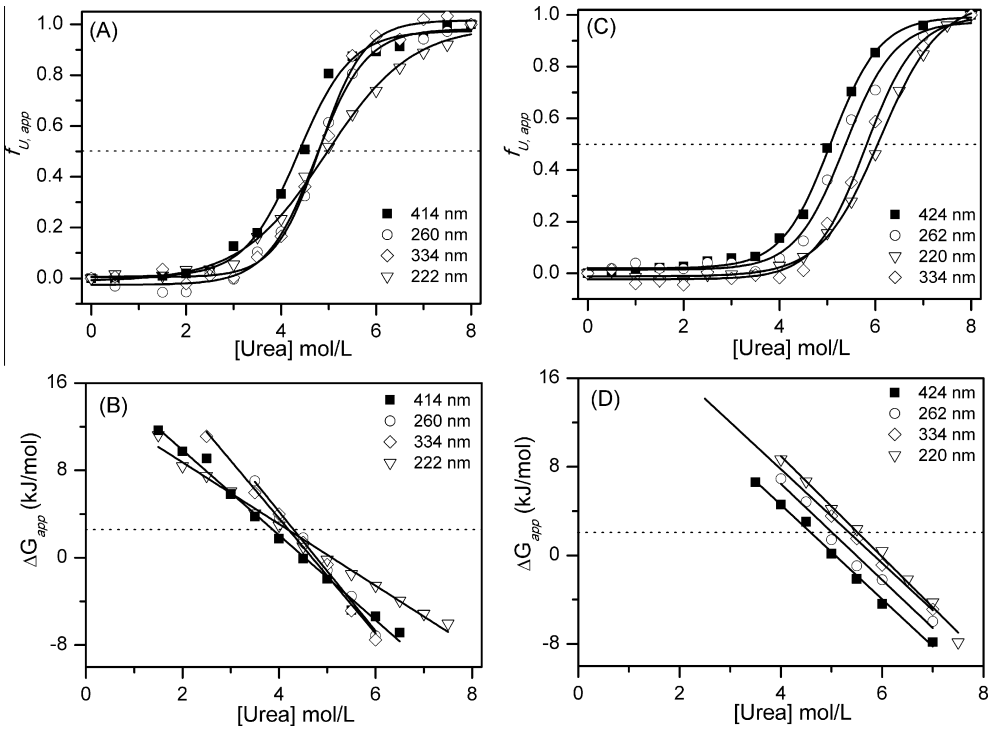

Fig. 6. Plots for the fraction of unfolded protein, $f_{U,app}$, as a function of urea concentration. The full lines correspond to fits to the two-state model described in Eqs. (3)–(6) (see "Methods"); the apparent unfolded fraction ($f_{U,app}$) based on CD data was calculated using Eq. (3). (A) oxy-HbGp (C) cyanomet-HbGp. (B) and (D) changes in free energy of the oxy- and cyanomet-HbGp forms as a function of urea concentration, respectively, at 298 K.

based on two different models to evaluate the adequacy of the simplest model and the need for more elaborate schemes, involving an intermediate state. In this paper, first, the results obtained from a two-state model are presented, followed by a discussion of the same data analyzed by a three-state model.

In Fig. 6A and B the fraction of denaturation ($f_{U,app}$) and the apparent free energy ($\Delta G_{U,app}$), as a function of urea concentration, associated with oxy-HbGp unfolding are shown. The values of r^2 ($r^2 > 0.991$) in Table 2 indicated that the obtained fits were quite reasonable. The values of $D_{1/2}$ of 5.1 ± 0.2 mol/L, ΔG_{H_2O} of 14.7 ± 0.4 kJ/mol and $-m$ of 2.9 ± 0.1 kJ/mol (mol/L)$^{-1}$ were obtained for urea denaturation, at pH 7.0, monitored at 222 nm (Table 2).

The values of $D_{1/2}$ at 222 nm obtained for oxy-HbGp, are larger than those observed for the other wavelengths (Table 2). These results suggest that, the stability in the heme group region towards urea is lower as compared to the peptide bonds, reflecting the protein secondary structure. In other words, the asymmetry of the heme group vicinity is disrupted more easily as compared to that associated to the HbGp folded structure. Moreover, the small value

Table 2
Thermodynamic parameters, obtained from spectroscopic data, associated with the urea induced denaturation of HbGp forms, at pH 7.0 and 25 °C by a two-state model.

Forms of the HbGp	Probe	$D_{1/2}$ [mol/L][a]	$-m$ [kJ/mol (mol/L)$^{-1}$][b]	$\Delta G_{H_2O,app}$ [kJ/mol][c]	r^2
Oxy-	FE[d]	5.2 ± 0.5	3.0 ± 0.6	15.6 ± 0.6	0.991
	LSI[e]	3.8 ± 0.7	4.4 ± 0.2	16.1 ± 0.5	0.996
	$[\theta]_{222\ nm}$	5.1 ± 0.2	2.9 ± 0.1	14.7 ± 0.4	0.992
	$[\theta]_{260\ nm}$	4.8 ± 0.1	4.9 ± 0.2	24 ± 1	0.993
	$[\theta]_{334\ nm}$	4.8 ± 0.1	4.8 ± 0.1	23.8 ± 0.5	0.992
	$[\theta]_{414\ nm}$	4.3 ± 0.1	3.9 ± 0.3	17.6 ± 0.5	0.990
Cyanomet-	FE[d]	5.6 ± 0.2	3.1 ± 0.3	17.2 ± 0.2	0.996
	LSI[e]	4.1 ± 0.3	4.3 ± 0.4	17.7 ± 0.4	0.998
	$[\theta]_{220\ nm}$	6.1 ± 0.1	4.2 ± 0.1	25.5 ± 0.4	0.992
	$[\theta]_{262\ nm}$	5.4 ± 0.1	4.3 ± 0.3	24 ± 2	0.992
	$[\theta]_{334\ nm}$	5.8 ± 0.1	4.2 ± 0.2	24.8 ± 0.2	0.995
	$[\theta]_{424\ nm}$	5.1 ± 0.1	4.3 ± 0.1	22 ± 1	0.997
Met-	$[\theta]_{262\ nm}$	1.93 ± 0.07	nd	nd	nd
	$[\theta]_{374\ nm}$	1.78 ± 0.05	nd	nd	
	$[\theta]_{414\ nm}$	1.95 ± 0.02	nd	nd	nd
		6.4 ± 0.2	nd	nd	

[a] Midpoint of the unfolding curve.
[b] The slope of plots of $\Delta G_{U,app}$ versus denaturant concentration.
[c] ΔG_{H_2O} is the intercept of plots of $\Delta G_{U,app}$ versus urea concentration at 0.0 mol/L denaturant.
[d] Parameters obtained from the analysis of data of the maximum area of fluorescence emission.
[e] Parameters obtained from the analysis of data of light scattering intensity (LSI).

Table 3
Thermodynamic parameters, obtained from spectroscopic data, associated with the urea induced denaturation of HbGp forms, at pH 7.0 and 25 °C, by a three-state model.

Forms of the HbGp	Probe	$([D]_{1/2})_1$ [mol/L][a,e]	$([D]_{1/2})_2$ [mol/L][a,f]	$-m_1$ [kJ/mol (mol/L)$^{-1}$][b,e]	$-m_2$ [kJ/mol (mol/L)$^{-1}$][b,f]	ΔG_1 [kJ/mol][e]	ΔG_2 [kJ/mol][f]	ΔG_3 [kJ/mol][g]
Oxy-	FE[c]	–	5.2 ± 0.2	–	2.7 ± 0.1	–	14 ± 1	–
	LSI[d]	3 ± 1	4.2 ± 0.2	3 ± 1	5 ± 1	9 ± 5	21 ± 1	30 ± 6
	$[\theta]_{222\ nm}$	3 ± 2	4.8 ± 0.1	4 ± 2	3.1 ± 0.1	12 ± 8	15 ± 2	27 ± 10
	$[\theta]_{260\ nm}$	3 ± 2	4.7 ± 0.1	1.0 ± 0.7	4.7 ± 0.5	3 ± 4	22 ± 2	25 ± 6
	$[\theta]_{334\ nm}$	3 ± 12	4.9 ± 0.1	7 ± 13	5.1 ± 0.5	21 ± 45	25 ± 3	–
	$[\theta]_{414\ nm}$	1 ± 1	4.3 ± 0.2	10 ± 5	4.8	6 ± 5	21 ± 2	27 ± 7
Cyanomet-	FE[c]	–	5.7 ± 0.3	–	3.0 ± 0.2	–	17 ± 2	–
	LSI[d]	1.8 ± 0.7	4.6 ± 0.2	8 ± 3	3.3 ± 0.2	14 ± 3	15 ± 1	29 ± 4
	$[\theta]_{220\ nm}$	4 ± 2	6.2 ± 0.2	6 ± 4	4.7 ± 0.4	22 ± 20	29 ± 3	–
	$[\theta]_{262\ nm}$	1 ± 5	5.1 ± 0.2	8 ± 14	5.3 ± 0.3	11 ± 20	27 ± 2	–
	$[\theta]_{334\ nm}$	3 ± 8	5.8 ± 0.1	6 ± 10	4.3 ± 0.3	18 ± 25	25 ± 2	–
	$[\theta]_{424\ nm}$	2 ± 1	5.1 ± 0.1	8 ± 6	5.1 ± 0.2	12 ± 10	26 ± 1	38 ± 11
Met-	$[\theta]_{262\ nm}$	1.85 ± 0.04	6 ± 7	9.1 ± 0.6	6 ± 7	17 ± 2	38 ± 40	–
	$[\theta]_{374\ nm}$	1.74 ± 0.05	4 ± 7	8.6 ± 0.8	4 ± 2	15 ± 1	14 ± 20	–
	$[\theta]_{424\ nm}$	–	–	–	–	–	–	–

[a] Critical denaturant molarity (urea).
[b] The parameter that shows the dependence of free energy of Gibbs with the concentration of denaturant.
[c] Parameters obtained from the analysis of data of the maximum area of fluorescence emission.
[d] Parameters obtained from the analysis of data of light scattering intensity (LSI).
[e] Thermodynamic parameters of first transition ($N \rightarrow I$).
[f] Thermodynamic parameters of second transition ($I \rightarrow U$).
[g] Total free energy of Gibbs obtained from the sum of the first transition, state native to intermediate, (ΔG_1) and the second transition, intermediate to unfolding state (ΔG_2).

of $-m$, at 222 nm, indicated that the oxy-HbGp denaturation is characterized by a small cooperativity.

Three-state model. The main results obtained from the analysis by a three-state model (see Eq. (8) in Methods section) are shown in Table 3. The values of the parameters $([D_{1/2}])_2$, m_2 and ΔG_2, for the second transition, found by the three-state model fittings are similar to those obtained previously by the two-state model (Table 2) for all techniques discussed in this paper. However, the corresponding values for the first transition, from native (N) to intermediate states (I), present, in many cases, data with very large errors (Table 3). For some probes, as, for example, FE (not shown) and CD at 334 nm, the values for the parameters $([D_{1/2}])_1$, m_1 and ΔG_1, due to these large estimated errors, are not reliable (absolute values comparable to errors, see Table 3). This first transition is a subtle one, probably, associated to partial protein oligomeric dissociation, and difficult to detect due to the strong similarity of the intermediate state to the native one. As a consequence, the ill defined corresponding plateau, precludes the precise determination of the parameters for this transition. Moreover, the analysis by the three-state model indicates that the transition around 4.3–5.2 mol/L of urea, associated to protein denaturation, is consistent with data obtained from the two-state analysis.

Our results show that, although the oxy-HbGp denaturation process can be fitted with the two state model [24,16,40,41], this is only a reasonable approximation, since the thermodynamic parameters obtained by the two models (for the second transition) are very consistent and converge to similar values (see Tables 2 and 3). However, the three-state model analysis is able to reveal a partial HbGp oligomeric dissociation, involving an intermediate state, which is very similar to the native one. Furthermore, these analyses are relevant, since they provide important information on the thermodynamic parameters for the protein denaturation, and, they can be used also for comparison of the stability of the different protein oxidation forms.

Cyanomet-HbGp

Two-state model. The CD spectra for the cyanomet-HbGp are very similar to those for the oxy-HbGp, indicating that both oxidation forms have similar α-helix structure contents. The fraction of denaturation and the free energy at 220 nm are displayed in the Fig. 6C and D. The critical urea concentration $D_{1/2}$ for cyanomet-HbGp, in the peptide region, is 6.1 ± 0.1 mol/L and a value of $-m$ of 4.2 ± 0.1 kJ/mol (mol/L)$^{-1}$, is obtained (Table 2). The free energy ΔG_{H_2O}, at 220 nm, associated with the stability of the cyanomet-HbGp in water is 25.5 ± 0.4 kJ/mol (Fig. 6D and Table 2).

In the heme region, the values of these parameters monitored at 420, 262 and 334 nm are smaller than those observed at 220 nm (Table 2). This behavior is similar to that found for oxy-HbGp. However, the values of $D_{1/2}$ and ΔG_{H_2O} are larger than those obtained for oxy-HbGp. Thus, our results show that the cyanomet-HbGp, in the presence of urea, is more stable than the oxy-HbGp. Besides, up to 4.0 mol/L of urea, the CD spectra remain practically unchanged (data not show). The high stability of cyanomet-HbGp is due to the coordination of the CN^- to the iron heme, since this ligand shows a greater tendency to accept π electrons from the heme iron as compared to the coordinated water. This interaction results in a trans-stabilization of the Fe^{3+}–His 93 bond [32]. Our results indicate that the secondary structure, monitored in the peptide region (220–222 nm), is more stable than that observed in the heme group (420 nm) and aromatic region (260 nm) environments. Besides, the tertiary and quaternary structures are less stable than the protein secondary structure, being more sensitive to the changes induced by increasing urea concentrations.

The cyanomet-HbGp also presents some changes in the values of the thermodynamic parameters, monitored at different wavelengths and probes (see Table 2), suggesting that the two-state model used in the analysis of this oxidized HbGp form is also an approximation. Moreover, for all analyzed wavelengths the values of $D_{1/2}$ for cyanomet-HbGp were larger, due to its higher oligomeric stability. The high stability of the cyanomet-HbGp was also observed in previous studies, involving surfactants, high temperatures and alkaline pH [3,12].

Three-state model. The results obtained for cyanomet-HbGp, in a similar way as for the oxy-form described above, also show very consistent thermodynamic parameters for both models (see Tables 2 and 3). Thus, as observed for the oxy-HbGp, the second transition, associated to protein denaturation, is characterized by $([D_{1/2}])_2$, m_2 and ΔG_2 values, that are very consistent with those

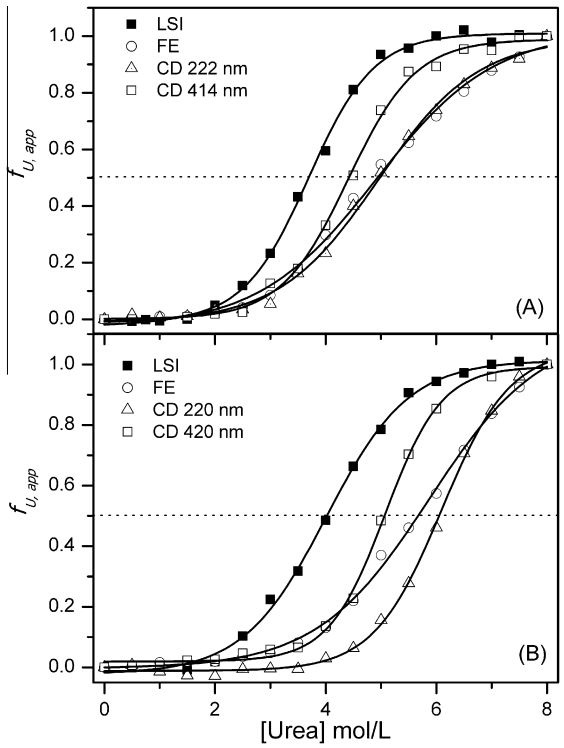

Fig. 7. (A) Ellipticity at 424 nm for cyanomet-HbGp 3.0 mg/mL, in 20 mmol/L phosphate buffer, at pH 7.0, in the presence of urea in the range 0.0–8.0 mol/L. Experimental data are given by open squares. The full line corresponds to the best fit using the two-state model, and the dashed line represents the fit by a three-state model. (B) Ellipticity at 262 nm for cyanomet- and met-HbGp forms, using the three-state model for data fit. The open circles and open triangles correspond to the experimental data for the cyanomet- and met-HbGp forms, respectively. Dashed lines correspond to the best fits.

obtained from the two-state model analysis, suggesting that the two-state model is a reasonable approximation. As discussed above, for oxy-HbGp, fittings based on the three-state model show that the first transition, at lower urea concentrations (1.0–3.0 mol/L), associated to partial oligomeric dissociation presents also great uncertainties regarding the thermodynamic parameters. In this case, the intermediate state is again very similar to the native one.

Fig. 7A displays the fits using both the two-state and three state models, for a particular data set of ellipticity at 424 nm, for cyanomet-HbGp, as a function of urea concentration, showing the consistency between the two models (see Tables 2 and 3).

Met-HbGp

In the CD analyses of met-HbGp it was not possible to determine all the thermodynamic parameters but only the critical urea concentrations. The denaturation process in this case could not be described by a two-state model. All the met-HbGp collected data suggest that a different dissociation/denaturation mechanism, as compared to the other two HbGp forms, takes place, corresponding to a more complex process. In the met-HbGp the iron is in the oxidation state Fe^{3+} with a water molecule coordinated to the metal at the sixth coordination position. Recent studies in our laboratory suggest that the aquomet-HbGp is less stable when exposed to several types of stress, such as the presence of surfactant, increase of temperature, increase of pH and addition of urea [3,12,21]. The loss of ellipticity for the met-HbGp is more intense than in the oxy- and cyanomet-HbGp forms, indicating that the met-HbGp presents a denaturation process different and less cooperative (data not shown). Moreover, 13% increase in the ellipticity is observed, at 0.5 mol/L of urea, associated with an increase of protein secondary structure. Data in the literature show that urea, at small concentrations, can induce the formation of secondary structure and increase the protein stability [42].

The CD spectra of met-HbGp, in the heme region, in the presence of urea, up to 8.0 mol/L, at pH 7.0, display smaller intensity in the Soret band as compared with the other two forms, suggesting that the water ligand induced changes in the symmetry of the heme group that originates the optical activity. The data at 262 and 374 nm show a similar behavior, and the estimated critical urea concentrations are 1.93 ± 0.07 and 1.78 ± 0.05 mol/L, respectively (Table 2, obtained at $f_U = 0.5$). The spectral changes are quite steep, indicating that the met-HbGp is the most unstable of all HbGp oxidation forms [3,12]. In the heme region, at 414 nm, two transitions are observed with the increase of the urea concentration: a first transition occurs at 1.95 ± 0.05 mol/L and a second one at 6.4 ± 0.2 mol/L (Table 2). These transitions can be associated to conformational changes in the vicinity of the heme, and they are well correlated to our optical absorption data, presented above, showing that, at 2.0 mol/L of urea, the formation of hemichrome is observed, while further increase in the urea concentration promotes the formation of a penta-coordinated species [21]. The very small variation in signal ellipticity in the urea concentration range 2.0–5.0 mol/L is due to the formation of a very stable hemichrome species.

Three-state model. Fitting the experimental data with the three-state model, made it possible to obtain some thermodynamic parameters for met-HbGp. Analyses were made for CD data, at two wavelengths (262 and 374 nm) and the results are also shown in Table 3. The values $([D_{1/2}])_1$ for both wavelengths are around 1.8 ± 0.1 mol/L of urea, indicating a smaller stability of this HbGp form. This transition corresponding to the formation of a hemichrome is very sharp and suggests that the hemichrome is associated to the intermediate state. So, a dramatic difference is noticed regarding the intermediate state for the three studied forms: in the case of oxy- and cyanomet-HbGp the intermediate state seems to be quite similar to the native one; for met-HbGp, apparently, the intermediate state is closer to the unfolded state. As a result, for met-form, the second transition is not very steep, and for this reason it was difficult to obtain reasonable thermodynamic parameters (very large errors, see Table 3). The formation of the hemichrome from aquomet-HbGp (at 1.0–2.0 mol/L of urea) drives the protein to an essentially denatured state. This result is illustrated in Fig. 7B, where met- and cyanomet CD data are compared, at the same wavelength of 262 nm. It is clear, that for all protein forms, two transitions are observed, a first one involved with oligomeric dissociation and a second one due to protein denaturation.

Protein concentration

It is worthy of notice, that in this paper, a detailed study of the effects of protein concentration on the stability, in the presence of urea, was not performed. In optical absorption, fluorescence emission and light scattering studies, described above, the protein concentration was fixed at 0.1 mg/mL. Furthermore, the protein concentration used in CD studies was fixed at 0.3 mg/mL for the peptide bonds spectral region and 3.0 mg/mL for the heme and aromatic aminoacids one. Previous HbGp temperature stability studies [12] have shown that the increase in protein concentration leads to higher protein stability. The different concentrations used in the present study are due to the sensitivity of the corresponding techniques. Besides, as our Tables 2 and 3 demonstrate, the thermodynamic parameters report the different sensitivities of the probes to the presence of increasing urea concentrations. For example, the sensitivity of the heme group is not expected to be the same as that of the tryptophan residues or the overall secondary structure. The probe specificity is well reflected in the differ-

ences of the parameters as a function of the technique and protein form.

An attempt was also performed to use optical spectroscopic techniques to evaluate the effect of protein concentration, in the limited range allowed by the optical techniques (light scattering and fluorescence emission), on the unfolding reaction. Fig. S2 of the Supporting information shows data for the light scattering, measured for oxy-HbGp, in the protein concentration range from 0.05 to 0.25 mg/mL. As can be seen the differences are not so great and a slight decrease of the critical urea concentration at the lower protein concentrations is observed. In Table S1 the thermodynamic parameters obtained from these experiments are collected together. Overall, in this limited protein concentration range the parameters are very similar within the estimated errors.

General discussion

Our studies on the stability of HbGp, in the presence of urea, indicate that the denaturation process depends on two factors: the iron oxidation state and the specific ligand coordinated to the iron. Significant differences in the denaturation process were observed for the three forms of HbGp studied in the present work. Thus, optical absorption, emission fluorescence and LSI show that the oxy- and cyanomet-HbGp are stable, up to 4.0 mol/L of urea, and at 8.0 mol/L of denaturant the protein is completely unfolded (see Fig. 8). Our optical absorption results suggest that the equilibria, in the presence of urea, for the oxy- and cyanomet-forms, are characterized by several species, formed both from the oxidation of the iron and the changes of ligands coordinated to the metal center. Analysis of these two forms by the three-state model revealed the existence of two transitions, a subtle one, at low urea concentrations, and a second one, more prominent, due to protein unfolding. The met-HbGp is the less stable of the three forms, and the equilibrium, in the studied urea concentration range, is described by two transitions, centered around 1.5 and 5.5 mol/L of urea, respectively. These transitions are due to the initial conversion of the aquomet-HbGp species into a hemichrome, which is, probably, associated to oligomeric dissociation, followed by a second transition involving the conversion of the hemichrome species into a penta-coordinated one, and linked to the protein unfolding.

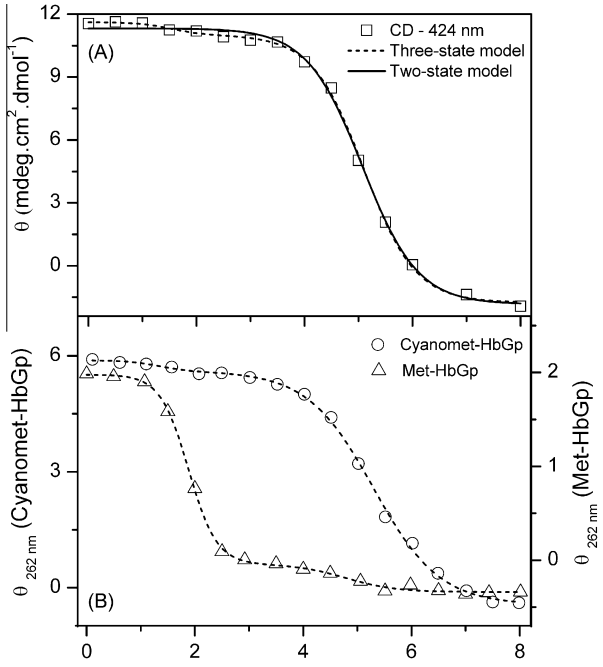

Fig. 8. $f_{U,app}$ curves for urea induced HbGp unfolding, obtained from light scattering intensity (LSI), fluorescence emission (FE), and circular dichroism (CD) data analysis. The full line is a fit to the two-state model described in Eqs. (3)–(6) (see "Methods"); (A) oxy-HbGp and (B) cyanomet-HbGp. (■) LSI, (○) FE, (Δ) peptide region CD and (□) heme region CD.

It is important to emphasize that the small values of $D_{1/2}$ obtained by LSI data as shown in Fig. 8 (see also Tables 2 and 3) as compared to the other techniques, strongly suggests that the oligomeric dissociation process occurs at lower concentrations of urea as compared to the protein denaturation. The LSI has a direct dependence on the volume of the scattering particles in solution, being an adequate technique to monitor the dissociation process. This result of partial dissociation of HbGp, as monitored by LSI, at lower concentrations of urea in the range 2.0–4.0 mol/L, is in excellent agreement with analytical ultracentrifugation data, where partial oligomeric dissociation of oxy-HbGp into smaller subunits was observed (data not shown).

The thermodynamic analysis, based on the spectroscopic data presented in this work, shows that, the two-state model adequately describes the main transition associated to the protein denaturation, for both oxy- and cyanomet-HbGp forms. The difference of stabilities of the two forms is evident when some specific spectral regions are compared. Thus, the ΔG_{H_2O} values for the Soret band, for oxy- and cyanomet-forms, are 17.6 ± 0.5 and 22 ± 1 kJ/mol, respectively (Table 2). A 4.4 kJ/mol increase in stability is noticed, in this case, for cyanomet-HbGp. Comparison of the peptide region shows an even greater increase in stability, with a 10.8 kJ/mol increase for cyanomet-HbGp. The order of stability observed for the three forms was: cyanomet- > oxy- > met-HbGp. The analysis of the same set of experimental data, based on a three-state model, with a general intermediate state of undefined stoichiometry [26,27], has allowed to improve the fittings of the data, revealing a second transition, at lower urea concentrations, where the intermediate state is very similar to the native one (see Fig. 7A and Table 3). Despite the large errors in the values of the parameters for this transition (Table 3), its existence could only be revealed by the three-state model analysis. Furthermore, the analysis for met-HbGp data has shown that the transition, at low concentrations of urea, is the main process detected for this protein form. In this case, the three-state model analysis suggests a great similarity of the intermediate state with the unfolded one. Therefore, formation of hemichrome induces oligomeric dissociation, facilitating the protein denaturation.

The oligomeric structure of HbGp is composed of 12 equal protomers $(\boldsymbol{abcd})_3\boldsymbol{L}_3$, involving seven different chains, four globins ***a***, ***b***, ***c*** and ***d***, and three linkers $\boldsymbol{L}_1$, $\boldsymbol{L}_2$ and $\boldsymbol{L}_3$. The whole oligomer consists of 144 globins and 36 linkers. Moreover, HbGp tetramer ***abcd*** consists of a disulfide bonded trimer ***abc*** and a monomer ***d***, a structure which is quite different as compared, for instance, with human hemoglobin where the tetramer is based on a pair of two different subunits, α and β. Thus, any appropriate stoichiometric model to describe the unfolding of HbGp should consider the dissociation of all chains of the oligomeric structure.

Reviewing the recent literature regarding protein denaturation induced by external agents such as chaotropic agents or temperature, some treatments comparing the two-state and three-state models are found, but generally, only very simple equilibria are considered for proteins undergoing either dimerization or dissociation of the dimer into monomers [43,44]. These models consider the formation of intermediates that are associated either to the dissociated monomer or to a dimeric form with a structure different from the native dimer, but not denatured [43–45]. The fully denatured protein involves the dissociation into monomers. Moreover, the reported studies on the stability of multimeric proteins [46,47] consider the denaturation of an *n*-mer protein into

monomers [46]. Again the unfolding reaction is of order n and its simplification involves some prior knowledge of the reaction stoichiometry and the concentration of the subunits produced upon dissociation. The same is true for the unfolding of a trimeric system described in [47]. Thus, these models are also not adequate to describe the denaturation process of HbGp, since for this protein the intermediate state is certainly a mixture of several species. An interesting alternative, which is presently under study in our laboratory, is the analysis of the equilibrium of different species of HbGp, in the presence of increasing concentrations of urea, by analytical ultracentrifugation. Preliminary observations for oxy-HbGp, at pH 7.0, show the appearance of the dodecamer subunit $(\boldsymbol{abcd})_3$ at low urea concentrations below 4.0 mol/L. This observation supports our suggestion that the subtle transition, at low concentrations of urea, could be due to partial oligomeric dissociation of the whole protein. The large errors associated to the thermodynamic parameters for this transition (Table 3) are, probably, due to the specificity of protein changes detected by the different probes used in this study, and, to some extent, also to the different species associated to the intermediate state along the unfolding pathway. This result is consistent with observations reported in the literature for hemoglobin of *L. terrestris* (HbLt) [48]. In summary, thermodynamic analysis by two-state and three-state models has allowed to obtain a significant amount of information regarding the three forms of HbGp. Two phenomena are coupled together in the denaturation process, oligomeric dissociation and unfolding. An intermediate state is formed of yet unknown structure that in the case of oxy- and cyanomet-HbGp is very similar to the native state, while for met-HbGp it resembles the unfolded state.

As mentioned above (see also [5]), there is still a long way before a complete denaturation model can be proposed for HbGp, due to the complexity of the system involving four globin and three linker subunits. This is certainly a very interesting matter for future work.

Conclusions

The present study of the urea effects upon HbGp contributes to the understanding of the protein stability in the presence of a denaturing agent. The denaturation and dissociation processes are very different and depend strongly on the iron oxidation forms and the ligand at the sixth coordination.

Our results suggest that the oxy- and cyanomet-HbGp forms present quite similar dissociation and denaturation processes, with a higher stability of the cyanomet-HbGp. The increase in the urea concentration induces the iron oxidation in the oxy-HbGp and the formation of other oxidized species. Analysis of the spectroscopic data based on a three-state model allowed to estimate the thermodynamic parameters for the two transitions observed: a first one, due to partial oligomeric dissociation, and a second one, associated to protein denaturation. Addition of urea also induces two transitions in the met-HbGp. Initially, in the low urea concentration range, between 1.0 and 2.0 mol/L, the dissociation of the oligomeric structure is observed, accompanied by the formation of a hemichrome species. For met-HbGp, and differently from oxy- and cyanomet-HbGp, this is the main transition observed in the spectroscopic data. At larger urea concentrations, a subtle decrease of secondary and tertiary structures is observed, due to the protein denaturation. The complete oligomeric dissociation is observed for both oxy- and cyanomet-HbGp forms, only at higher concentrations of urea (above 4 mol/L) together with denaturation. All the techniques used in this work indicate that the order of stability of the HbGp forms is given by cyanomet- > oxy- > met-HbGp.

The thermodynamic parameters associated to the unfolding of the oxy- and the cyanomet-HbGp forms, determined based on the two-state model, are very similar to those obtained from the three-state model main transition. For the met-HbGp the two-state model was not adequate to fit the data, but gave quantitative values similar to those obtained from the three-state model fits. The use of two-state and three state models analysis of experimental data allowed to underline the existence of an intermediate state, which is similar to the native state for both oxy- and cyanomet-HbGp, while for met-HbGp it is similar to the unfolded protein state. Formation of hemichrome from aqueous met-HbGp, at low urea concentrations, seems to facilitate both oligomeric dissociation and protein denaturation.

In summary, urea at low concentrations up to 4.0 mol/L, induces the partial dissociation of the oligomeric structure without large changes in the heme group, secondary and tertiary structures, for oxy- and cyanomet-HbGp. Further increase in the urea concentration, above 4.0 mol/L, causes the oxidation of the iron and the denaturation of the protein. For met-HbGp, low concentrations of urea induce dramatic changes of the oligomeric protein structure.

Acknowledgments

The authors are grateful to the Spectroscopy and Calorimetric Laboratory (LEC), CTN-Bio, Campinas, Brazil, for making available the CD equipment used in this work. Thanks are also due to the Brazilian agencies FAPESP, CNPq, and CAPES for partial financial support. P.S. Santiago is grateful to CNPq and FAPESP for postdoctoral grants. F.A.O. Carvalho is the recipient of a Ph.D. Grant from FAPESP (2009/17261-6). M. Tabak is grateful to CNPq for a research grant. Thanks are also due to Mr. Ézer Biazin for efficient support in sample preparations, and to Prof. J.C. Borges from our Institute for helpful discussions concerning the analysis of urea denaturation data using a three-state model.

Appendix A. Supplementary data

Supplementary data associated with this article can be found, in the online version, at doi:10.1016/j.abb.2012.01.007.

References

[1] F.A.O. Carvalho, P.S. Santiago, J.C. Borges, M. Tabak, Anal. Biochem. 385 (2008) 257–263.
[2] W.E. Royer, K. Strand, M. Van Heel, W.A. Hendrickson, Proc. Natl. Acad. Sci. 97 (2000) 7107–7111.
[3] S.N. Vinogradov, Micron 35 (2004) 127–129.
[4] M.S. Oliveira, L.M. Moreira, M. Tabak, Int. J. Biol. Macromol. 40 (2007) 429–436.
[5] F.A.O. Carvalho, P.S. Santiago, J.C. Borges, M. Tabak, Int. J. Biol. Macromol. 48 (2011) 183–193.
[6] R.E. Weber, S.N. Vinogradov, Physiol. Rev. 81 (2001) 569–628.
[7] W.E. Royer, H. Zhu, T.A. Gorr, J.F. Flores, J.E. Knapp, J. Biol. Chem. 280 (2005) 27477–27480.
[8] T. Harnois, M. Rousselot, H. Rogniaux, F. Zal, Artif. Cells Blood Sub. 37 (2009) 106–116.
[9] M. Rousselot, E. Delpy, C. Drieu La Rochelle, V. Lagente, R. Pirow, J-F. Rees, A. Hagege, D. Le Guen, S. Hourdez, F. Zal, Biotechnol J. 1 (2006) 333–345.
[10] F. Zal, B.N. Green, P. Martineau, F.H. Lallier, A. Toulmond, S.N. Vinogradov, J.J. Childress, Eur. J. Biochem. 267 (2000) 5227–5236.
[11] N.C. Meirelles, B. Oliveira, E. de Paula, S. Marangoni, G.M. Rennebeck, Comp. Biochem. Physiol. 88A (1987) 337–379.
[12] P.S. Santiago, J.W.P. Carvalho, M.M. Domingues, N.C. Santos, M. Tabak, Biophys. Chem. 152 (2010) 128–138.
[13] C.N. Pace, CRC Crit. Rev. Biochem. 3 (1975) 1–43.
[14] C.N. Pace, Methods Enzymol. 131 (1986) 266–280.
[15] C. Tanford, Adv. Protein Chem. 23 (1968) 121–282.
[16] F. Vanzi, B. Madan, K. Sharp, J. Am. Chem. Soc. 120 (1998) 10748–10753.
[17] P.S. Santiago, F. Moura, L.M. Moreira, M.M. Domingues, N.C. Santos, M. Tabak, Biophys. J. 94 (2008) 2228–2240.
[18] P.S. Santiago, L.M. Moreira, E.V. de Almeida, M. Tabak, Biochim. Biophys. Acta 1770 (2007) 506–517.
[19] A.L. Poli, L.M. Moreira, M. Tabak, H. Imasato, Colloids Surf. B 52 (2006) 96–104.

[20] S.C.M. Agustinho, M.H. Tinto, J.R. Perussi, M. Tabak, H. Imasato, Comp. Biochem. Physiol. 118A (1998) 171–181.
[21] S.C.M. Agustinho, M.H. Tinto, H. Imasato, T.T. Tominaga, J.R. Perussi, M. Tabak, Biochim. Biophys. Acta 1298 (1996) 148–158.
[22] A. Perczel, G.D. Fasman, Biophys. Chem. 48 (1993) 19–29.
[23] M. Beenu, H.Q. Shabir, A. Faizan, Biochim. Biophys. Acta 1646 (2003) 49–56.
[24] K.B. Devaraj, P.R. Kumar, V. Prakash, Process Biochem. 46 (2011) 458–464.
[25] R.M. Ionescu, V.F. Smith, J.C. O'Neill Jr., C.R. Matthews, Biochemistry 39 (2000) 9540–9550.
[26] H.C. Hung, G. Chang, Biophys. J. 81 (2001) 3456–3471.
[27] J.L. Soulages, Biophys. J. 75 (1998) 484–492.
[28] D.J. Tew, S.P. Bottomley, J. Mol. Biol. 313 (2001) 1161–1169.
[29] J.J. Guidry, C.K. Moczygemba, N.K. Steede, S.J. Landry, P. Wittung-Stafshede, Protein Sci. 9 (2000) 2109–2117.
[30] Y. Sugawara, A. Matsuoka, A. Kaino, K. Shikama, Biophys. J. 69 (1995) 583–592.
[31] A.L. Poli, L.M. Moreira, A.A. Hidalgo, H. Imasato, Biophys. Chem. 114 (2005) 253–260.
[32] M.S. Hargrove, J.S. Olson, Biochemistry 35 (1996) 11310–11318.
[33] E. Droghetti, S. Sumithran, M. Sono, M. Antalik, M. Fedurco, J.H. Dawson, G. Smulevich, Arch. Biochem. Biophys. 489 (2009) 68–75.
[34] A. Perczel, K. Park, G.D. Fasman, Anal. Biochem. 203 (1992) 83–93.
[35] P.S. Santiago, F.A.O. Carvalho, M.M. Domingues, J.W.P. Carvalho, N.C. Santos, M. Tabak, Langmuir 26 (12) (2010) 9794–9801.
[36] C.B. Cabral, H. Rosa, J.C. Imasato, H.J. Laure, C.H.T.P. Silva, M. Tabak, R.C. Garratt, L.J. Greene, Biophys. Chem. 97 (2002) 139–157.
[37] J. Ramprakash, V. Doseeva, A. Galkin, W. Krajewski, L. Muthukumar, S. Pullalarevu, E. Demirkan, O. Herzberg, J. Moult, F.P. Schwarz, Anal. Biochem. 374 (2008) 221–230.
[38] J.K. Myers, C.N. Pace, J.M. Scholtz, Protein Sci. 4 (1995) 2138–2148.
[39] S. Nallamsetty, V.K. Dubey, M. Pande, P.K. Ambasht, M.V. Jagannadham, Biochimie 89 (2007) 1416–1424.
[40] E.S. Cobos, V.V. Filimonov, A. Gálvez, E. Valdivia, M. Maqueda, J.C. Martínez, P.L. Mateo, Biochim. Biophys. Acta 1598 (2002) 98–107.
[41] F. Hailong, G. Grimsley, S.J. Martin, C.N. Pace, Protein Sci. 19 (2010) 1044–1052.
[42] L. Marcelo, F. Holthauzen, D.W. Bolen, Protein Sci. 16 (2007) 293–298.
[43] J.A.O. Rumfeldt, C. Galvagnion, K.A. Vassall, E.M. Meiering, Prog. Biophys. Mol. Biol. 98 (2008) 61–84.
[44] S.A. Hobart, D.W. Meinhold, R. Osuna, W. Colon, Biochemistry 41 (2002) 13744–13754.
[45] D.S. Sánchez-Miguel, J. Romero-Jiménez, C.A. Reyes-López, A.L. Cabrera-Ávila, N. Carrillo-Ibarra, C.G. Benítez-Cardoza, Protein J. 29 (2010) 1–10.
[46] C. Park, S. Marqusee, Protein Sci. 13 (2004) 2553–2558.
[47] J. Backmann, G. Schaffer, L. Wyns, H. Bonisch, J. Mol. Biol. 284 (1998) 817–833.
[48] A. Krebs, A.R. Kuchumov, P.K. Sharma, E.H. Braswell, P. Zipper, R.E. Weber, G. Chottard, S.N. Vinogradov, J. Biol. Chem. 271 (1996) 18695–18704.